21. Tajimi, H., "A Statistical Method of Determining the Maximum Response of a Building Structure during an Earthquake," Proc. Second World Conf. Earthq. Engrg., Tokyo and Kyoto, Japan, 1960.
22. Timoshenko, S. P., and Gere, J. M., *Theory of Elastic Stability*, 2nd ed., McGraw-Hill, New York, N.Y., 1961.
23. Westermo, B. D., "Gravity and Dynamic Response of Vertical Beams," *Journal of the Engineering Mechanics Division*, ASCE, Vol. 107, No. EM5, Oct., 1981.
24. Wang, M. C., and Uhlenbeck, G. E., "On the Theory of the Brownian Motion II," in *Selected Papers on Noise and Stochastic Processes*, ed. by N. Wax, Dover Publications, Inc., New York, N.Y., 1954.
25. Wirsching, P. H., and Yao, J.T.-P., "Random Behavior of Columns," *Journal of the Engineering Mechanics Division*, ASCE, Vol. 97, No. EM3, 1971.
26. Wong, E., *Stochastic Processes in Information and Dynamical Systems*, McGraw-Hill, New York, N.Y., 1971.
27. Yamamoto, S., and Suzuki, N., "Experimental and Theoretical Analysis of Response against Earthquakes of Tower Structures Having Non-Uniform Sections Governed by Bending Vibrations," Proc. Third World Conf. Earthq. Engrg., Auckland and Wellington, New Zealand, 1965.

Hybrid Model for Discrete Cracks in Concrete

By Daniel J. W. Wium,[1] A. M. ASCE, Oral Buyukozturk,[2] M. ASCE, and Victor C. Li,[3] M. ASCE

Abstract: A method is proposed for the analysis of mode I and mixed mode crack propagation in concrete. It is based on a hybrid technique which uses finite elements to represent the uncracked specimen, and distributed dislocations to represent the crack. Consequently, no remeshing of the finite elements is required after crack propagation. This method is improved and further developed to make it applicable to concrete by incorporating the nonlinear traction transfer characteristics in a crack in concrete. By incorporating expressions obtained from previous studies to represent the aggregate interlock and imperfect debonding (i.e., tensile softening) in the crack, the major sources of nonlinearity caused by cracking are accounted for. Crack propagation in a single edge notched beam, subjected to four point bending, is modeled correctly, while the predicted reduction in load corresponds satisfactorily with the experimentally obtained results.

Introduction

Cracking of concrete is known to play a significant role in the nonlinear behavior of concrete structures. Two methods are typically used to represent this behavior in finite element analyses. Originally, discrete cracks were modeled as discontinuities in the finite element mesh. Later, the smeared crack method was introduced to represent the development of microcracks in the body more accurately. Both these methods have certain disadvantages. In the first method, the geometry of the structure changes when the crack propagates, and requires a new finite element mesh, while in the latter case, discrete cracks cannot be modeled accurately.

In this paper, the application of a surface integral, finite element hybrid method for the analysis of discrete cracks is proposed. Linear elastic fracture mechanics concepts are used with the theory of dislocations and the finite element method to represent the presence of a discontinuity in a concrete specimen. The hybrid method was first proposed by Annigeri and Cleary (2) in the context of the fracture of linear elastic bodies and the formation of shear bands in granular materials. In the present work this method is adopted to model discrete cracks in concrete and further developed to incorporate traction transfer properties across a crack in concrete.

The following section gives a brief review of previous studies on the propagation of discrete cracks in concrete. The basic theory used in the

[1]Engr., Van Wyk and Louw Inc., P.O. Box 905, Pretoria, South Africa.
[2]Assoc. Prof., Civ. Engrg. Dept., Massachusetts Institute of Technology, Cambridge, Mass.
[3]Asst. Prof., Civ. Engrg. Dept., Massachusetts Institute of Technology, Cambridge, Mass.
Note.—Discussion open until January 1, 1985. To extend the closing date one month, a written request must be filed with the ASCE Manager of Technical and Professional Publications. The manuscript for this paper was submitted for review and possible publication on December 7, 1983. This paper is part of the ***Journal of Engineering Mechanics***, Vol. 110, No. 8, August, 1984. ©ASCE, ISSN 0733-9399/84/0008-1211/$01.00. Paper No. 19045.

proposed hybrid method is summarized next, and in that context different shear transfer models are reviewed. One of these models is incorporated in the proposed hybrid model to represent the behavior of cracked concrete more realistically. The developed method is applied to a beam with a single edge notch under shear loading and the results are reviewed. Finally, the advantages of the method over existing techniques are reviewed, and practical applications and future extensions are pointed out.

Fracture Mechanics Applied to Concrete

Many researchers have investigated the applicability of linear elastic fracture mechanics to crack propagation in concrete, and many conflicting results have been obtained. A comprehensive review of these investigations was given by Mindess (30).

Kaplan (27) was one of the pioneers in determining the critical strain energy release rate in notched concrete beams. He found that the concept of a critical strain energy release rate, proposed by Griffith (21), is applicable to concrete, but the actual rate depended on the size, geometry and loading of the specimen. Several other workers found similar results (refer to Ref. 30 for a summary of these tests). Kesler, Naus and Lott (28), for example, also found that the stress intensity factor varies with crack length. Subsequently, Saouma, Ingraffea and Catalano (35) pointed out that these experimental results should be analyzed with more recently obtained stress intensity factor calculations, in which case constant values for the critical stress intensity factor, K_{IC}, were obtained for different specimen geometries.

During the fracture process of concrete, the nonlinearity and nonhomogeneity of the material basically renders linear elastic fracture mechanics inapplicable to concrete. This can especially be ascribed to the microcracking in the region of the crack, and the slow crack growth (creep effects) prior to unstable crack propagation (7). In an early attempt to represent this behavior, Kesler, Naus and Lott (28) suggested that microcracking at the crack tip can be modeled by a plastic cracked strip. This approach was a variation of a model Dugdale (12) originally developed for yielding at crack tips in steel plates. It was assumed that tractions act in the crack which attempts to prevent the crack from opening. These tractions were assumed to be explicit functions of the distance from the crack tip, with no regard for the crack opening (Fig. 1(*a*)). Hillerborg, Modeer and Petersson (24) extended this formulation to incorporate the actual strain softening behavior in a crack, which had been recorded in a number of uniaxial tensile tests (14,22). Rather than assuming a specific stress distribution in the crack, a representative stress-displacement relation based on the experiments was used (Fig. 1(*b*)). The concrete was treated as a linear elastic material prior to cracking, but once it reached the tensile strength, the stress decreased with increasing crack width at a constant (negative) modulus. The problem becomes a nonlinear one and cannot be solved analytically. Petersson (33,34) and Gylltoft (20) implemented this technique in a finite element program, and satisfactorily predicted the behavior of various test specimens. Catalano and Ingraffea (8) extended this fictitious crack model by using a

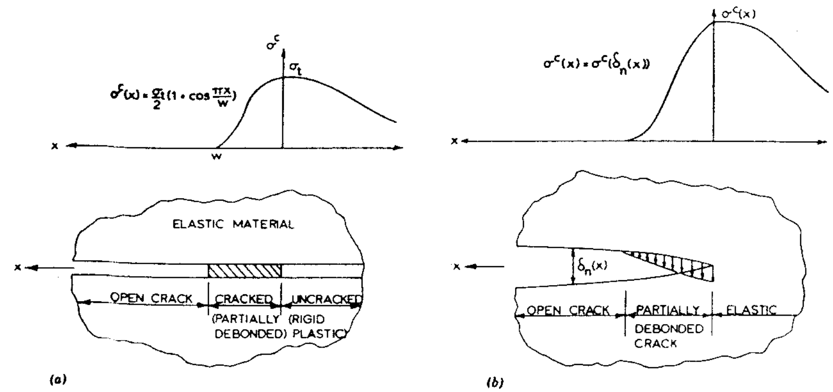

FIG. 1.—Numerical Models for Traction Transfer in Cracks: (*a*) Model Proposed by Kesler, Naus and Lott (28); and (*b*) Model Proposed by Hillerborg, Modeer and Petersson (24)

nonlinear unloading branch for the tensile stress-strain relation. This was incorporated in a finite element program in which quarter point singular, linear strain, isoparametric finite elements represented the strain and stress singularities at the crack tip. Link elements were used between the two sides of the crack to incorporate the crack face constitutive law. A similar method was used to include the effect of shear transfer across the crack in cases where pure mode I conditions did not apply. These methods have the disadvantage that a new finite element mesh has to be defined once the crack propagates.

Bazant and Cedolin (4) developed the blunt crack band method for linear elastic materials, and later Bazant and Oh (6) adapted it for concrete. It is assumed that the process zone at the crack is as wide as one finite element. Once a crack forms, the compliance of the element is modified to represent a softening, unloading branch. This stress-strain relation depends on the width of the chosen finite element (or process zone), the critical energy release rate and tensile strength of the material. The method has only been used for pure mode I analysis, and extension to mixed mode cases has not been touched upon. The method has the advantage that a new finite element mesh is not required after propagation, but certain limitation with regard to the crack size are implicitly or explicitly assumed.

Hybrid Method

A hybrid method, which combines the advantages of the finite element and boundary integral methods, was recently proposed for the analysis of cracks in finite bodies. This new approach utilizes finite elements to represent the features (particularly the finite geometry) of the body in which the crack occurs, while a continuous distribution of dislocations are used to model the crack (10). The effects of the dislocations are evaluated with a surface integral method. The crack can be treated as a pseudo-substructure in the body by assuming that superposition holds for the specimen. A generalized stiffness matrix is assembled, and the displacements and dislocation densities can be obtained explicitly. A brief review of the derivation of the generalized stiffness matrix is given in this section.

Assume that a linear elastic body, in which a crack exists, is subjected to boundary tractions **R** (Fig. 2). Tractions of magnitude **T** act on the crack. The actual stress and displacement fields in the body can then be treated as the superposition of two problems, by using the general method of substructuring. First, consider a crack with the same configuration as the actual problem, but in an infinite domain. Represent this crack by the superposition of mode I and mode II dislocations, distributed along the crack. Assume that tractions $\mathbf{T}^{si}$ act along this crack, which create certain stress and displacement fields in the infinite body. When the boundaries of the actual body are mapped onto the infinite body, the normal and shear tractions along this path can be calculated from the stress influence functions for dislocations. The corresponding equivalent nodal forces, $\mathbf{R}^{si}$, (which act on the finite body) can be calculated from these tractions as

$$\mathbf{R}^{si} = \mathbf{GF} \quad \text{(1)}$$

in which **G** = the traction influence matrix, and **F** = the dislocation density amplitudes (derivatives of the dislocations with respect to the distance along the crack). The surface tractions along the crack can also be written in terms of the dislocation density amplitudes as

$$\mathbf{T}^{si} = \mathbf{CF} \quad \text{(2)}$$

in which **C** = the matrix representing the stress influence functions along the crack.

The displacements (at the finite element nodes) due to the dislocations are given by the displacement influence functions. Special care has to be taken to represent the line of discontinuity of the crack correctly. These influence functions are used to compile the matrix **L**, which expresses

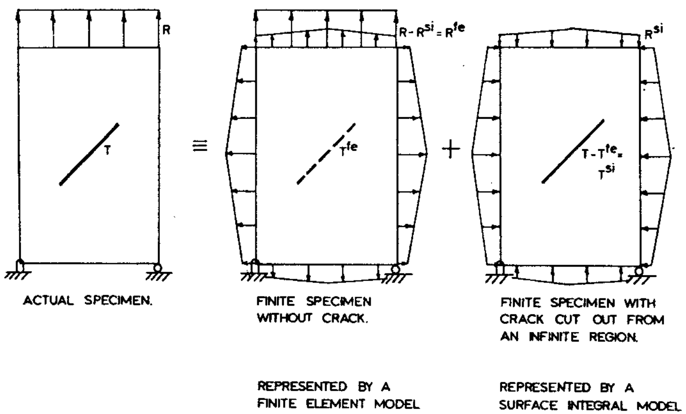

FIG. 2.—Schematic Representation of Hybrid Finite Element and Surface Integral Method for Analysis of Finite Specimens with Discrete Cracks

the displacements at the nodes in terms of the dislocation density amplitudes

$$\mathbf{U}^{si} = \mathbf{LF} \quad \text{(3)}$$

Consider also a finite body without a crack which is represented by finite elements and subjected to applied boundary tractions $\mathbf{R}^{fe}$. The displacements can be found from the well-known expression, $\mathbf{KU}^{fe} = \mathbf{R}^{fe}$, in which **K** = the stiffness matrix of the specimen. These displacements will in turn create stresses along the line of the crack that can be written as

$$\mathbf{SU}^{fe} = \mathbf{T}^{fe} \quad \text{(4)}$$

in which **S** = traction influence matrix. The total displacements (**U**) are the sum of the displacements due to the dislocations and the load vector $\mathbf{R}^{fe}$. Thus

$$\mathbf{U} = \mathbf{U}^{fe} + \mathbf{U}^{si} = \mathbf{U}^{fe} + \mathbf{LF} \quad \text{(5)}$$

The total applied load vector, **R** is

$$\mathbf{R} = \mathbf{R}^{fe} + \mathbf{R}^{si} = \mathbf{KU}^{fe} + \mathbf{GF} \quad \text{(6)}$$

and from Eq. 5,

$$\mathbf{R} = \mathbf{K}(\mathbf{U} - \mathbf{LF}) + \mathbf{GF} = \mathbf{KU} + (\mathbf{G} - \mathbf{KL})\mathbf{F} \quad \text{(7)}$$

Similarly, the tractions along the crack will be

$$\begin{aligned}\mathbf{T} &= \mathbf{T}^{fe} + \mathbf{T}^{si}\\ &= \mathbf{SU}^{fe} + \mathbf{CF}\\ &= \mathbf{SU} + (\mathbf{C} - \mathbf{SL})\mathbf{F} \quad \text{(8)}\end{aligned}$$

The global generalized stiffness matrix can be written as

$$\begin{bmatrix}\mathbf{K} & (\mathbf{G}-\mathbf{KL})\\ \mathbf{S} & (\mathbf{C}-\mathbf{SL})\end{bmatrix}\begin{bmatrix}\mathbf{U}\\ \mathbf{F}\end{bmatrix} = \begin{bmatrix}\mathbf{R}\\ \mathbf{T}\end{bmatrix} \quad \text{(9a)}$$

or

$$\begin{bmatrix}\mathbf{K} & \mathbf{G}^*\\ \mathbf{S} & \mathbf{C}^*\end{bmatrix}\begin{bmatrix}\mathbf{U}\\ \mathbf{F}\end{bmatrix} = \begin{bmatrix}\mathbf{R}\\ \mathbf{T}\end{bmatrix} \quad \text{(9b)}$$

The different matrices for the dislocations are set up by using Gauss-Chebychev integration along the crack. The influence functions for stress (which are used to calculate the **G** and **C** matrices) are well-known (23,31). Matrix **S** is calculated from the stress interpolation functions for the finite elements. Matrix **K** can be compiled in a number of ways, of which the finite elements technique is most convenient.

This set of linear equations has to be solved to obtain the displacements and dislocation density amplitudes. It should be noted that this stiffness matrix is not symmetric, and solving this particular form can be tedious and costly. A slightly improved method is to solve for the total displacements from the first expression in Eq. 9*b*, so that

$$\mathbf{U} = \mathbf{K}^{-1}(\mathbf{R} - \mathbf{G}^*\mathbf{F}) = (\mathbf{K}^{-1}\mathbf{R}) - (\mathbf{K}^{-1}\mathbf{G}^*)\mathbf{F} \quad \text{(10)}$$

Substituting this expression into the second expression in Eq. 9b, and solving for F, one obtains

$$\mathbf{F} = [\mathbf{C}^* - \mathbf{S}(\mathbf{K}^{-1}\mathbf{G}^*)]^{-1}[\mathbf{T} - \mathbf{S}(\mathbf{K}^{-1}\mathbf{R})] \quad (11)$$

Since K is a symmetric, banded matrix, the very efficient numerical methods that are available for the inversion of finite element stiffness matrices can be used to find the two products ($\mathbf{K}^{-1}\mathbf{G}^*$) and ($\mathbf{K}^{-1}\mathbf{R}$). The matrix $[\mathbf{C}^* - \mathbf{S}(\mathbf{K}^{-1}\mathbf{G}^*)]$ will generally be of much lower order than the original full stiffness matrix, and can be solved as usual. The total displacements can then easily be obtained from Eq. 10, since both large matrix multiplications have already been performed to solve Eq. 11.

The stress intensity factors at the crack tips can be calculated from the dislocation density amplitudes (11). If the critical stress intensity factor of the material (K_{IC}) is known, and it is assumed that crack extension will take place in a direction normal to the direction of maximum tensile stress (13), the load level required to propagate the crack can be calculated. The general approach to this problem is to extend the crack by a certain increment, and then calculate the loads corresponding to this extension. Since this is an incremental method, two different approaches can be followed to calculate the direction of crack extension. In the first method it is assumed that the stress field around the current crack tip (point A in Fig. 3) can be modeled with the normal expression for stresses at a crack tip. The new direction of a short crack increment will be in the direction where K_{II} is zero. Erdogan and Sih (13) pointed out that the relation between K_I and K_{II} is given by $K_I \sin\theta + K_{II}(3\cos\theta - 1) = 0$ where θ is the direction with respect to the previous crack direction in which K_{II} will be zero (Fig. 3). The value of θ can be calculated from this expression when K_I and K_{II} are known.

The second alternative is to find the direction in which the crack must extend so that the value of K_{II} is zero at the new tip (point B). In a body in which the direction of the principal stresses change from point to

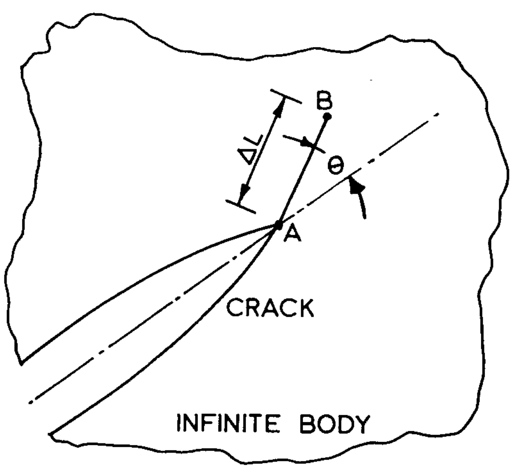

FIG. 3.—Crack Extension from Present Configuration

point, this direction will depend upon the incremental length (Δ.) of the crack. These two methods will converge to the same crack path when shorter crack increments are used. Both methods have been used, but it was found that the explicit nature of the first technique required significantly less computer time than the second iterative method.

Crack Face Tractions

In the previous derivation, it was assumed that the tractions acting on the crack faces (T) are independent of the relative displacements in the crack. This is usually the case for externally applied pressures in the crack. In many materials, though, the two faces of the crack still remain in partial contact and some material ligaments even remain unbroken and span the crack. In that case the crack fact tractions are functions of the relative displacement in the crack and consequently the set of governing equations becomes nonlinear. This is particularly true for concrete where aggregate interlock and tension softening in a crack depend on the crack opening [Petersson (33)].

Although the constitutive relations of the two phenomena of aggregate interlock and tension softening are vastly different, it will be assumed that the influence functions for tractions along the crack will be independent of the source of these tractions. The particular constitutive relations, which express the stresses along the crack in terms of the relative crack displacements, are discussed in the following section. In this section, a procedure is proposed for the solution of the general set of nonlinear equations. Generally, these crack face tractions are load path dependent. Due to the lack of sufficient experimental data to formulate the overly complex model that will be needed to incorporate all the significant features, it will be assumed that the stresses are path independent. In that case, the stresses across the crack ($\mathbf{T}_{cr}$) are functions of the relative displacement of the crack faces ($\mathbf{U}_{cr}$) or

$$\mathbf{T}_{cr} = \mathbf{T}_{cr}(\mathbf{U}_{cr}) \quad (12)$$

The relative crack displacements ($\mathbf{U}_{cr}$) are in turn linear functions of the dislocation densities along the crack, or

$$\mathbf{U}_{cr} = \mathbf{DF} \quad (13)$$

in which $\mathbf{D}$ represents the displacement influence functions along the crack. The crack surface tractions can then be written in terms of the dislocation density amplitudes

$$\mathbf{T}_{cr} = \hat{\mathbf{T}}_{cr}(\mathbf{DF}) = \mathring{\mathbf{T}}(\mathbf{F}) \quad (14)$$

Let the total tractions on the crack surface be the sum of the externally applied tractions, $\mathbf{T}_a$, and those tractions $\mathbf{T}_{cr}$ that exist due to the particles spanning the crack. The traction vector in Eq. 11 can then be expressed as

$$\mathbf{T} = \mathbf{T}_a + \mathbf{T}_{cr} \quad (15)$$

Eq. 11 can be rewritten as

$$[\mathbf{C}^* - \mathbf{S}(\mathbf{K}^{-1}\mathbf{G}^*)]\,\mathbf{F} = \mathbf{T}_a + \mathring{\mathbf{T}}_{cr}(\mathbf{F}) - \mathbf{S}(\mathbf{K}^{-1}\mathbf{R}) \quad (16a)$$

or in abbreviated form as

$$\mathbf{C}_e\mathbf{F} = \mathring{\mathbf{T}}_{cr}(\mathbf{F}) + \mathbf{T}_e \quad (16b)$$

This is a nonlinear equation which, in general, cannot be solved explicitly. The Newton-Raphson method will be used to solve this expression. If a new function is defined as

$$\phi(\mathbf{F}) = \mathbf{C}_e\mathbf{F} - \mathring{\mathbf{T}}_{cr}(\mathbf{F}) - \mathbf{T}_e \quad (17)$$

the solution of Eq. 16*a* corresponds to the solution of the expression

$$\phi(\mathbf{F}) = 0 \quad (18)$$

The first two terms of the Taylor series expansion for this function are

$$\phi(\mathbf{F}^i + \Delta\mathbf{F}^i) = \phi(\mathbf{F}^i) + \frac{d\phi}{d\mathbf{F}}\Delta\mathbf{F}^i + \ldots$$

An improved estimate $\mathbf{F}^{i+1}$ for the solution of the equation $\phi(\mathbf{F}^{i+1}) = 0$ can be calculated from the previous estimate $\mathbf{F}^i$

$$\mathbf{F}^{i+1} = \mathbf{F}^i + \Delta\mathbf{F}^i$$

By ignoring any higher order terms

$$\frac{d\phi}{d\mathbf{F}}\Delta\mathbf{F}^i = -\phi(\mathbf{F}^i) \quad (19)$$

Here, $d\phi/d\mathbf{F}$ can be treated as an effective tangent stiffness matrix. For this formulation

$$\frac{d\phi}{d\mathbf{F}} = \mathbf{C}_e - \frac{d\mathring{\mathbf{T}}_{cr}(\mathbf{F})}{d\mathbf{F}} \quad (20)$$

Let **E** be a matrix expressing the incremental crack tractions, $\Delta\mathbf{T}_{cr}$, in terms of the incremental crack displacements, $\Delta\mathbf{U}_{cr}$ such that

$$\Delta\mathbf{T}_{cr} = E\Delta\mathbf{U}_{cr} = \mathbf{ED}\Delta\mathbf{F} \quad (21)$$

Eq. 19 then becomes

$$[\mathbf{C}^* - \mathbf{S}(\mathbf{K}^{-1}\mathbf{G}^*) - \mathbf{ED}]\,\Delta\mathbf{F}^i = -[\mathbf{C}^* - \mathbf{S}(\mathbf{K}^{-1}\mathbf{G}^*)]\,\mathbf{F}^i + \mathring{\mathbf{T}}_{cr}(\mathbf{F}^i) + \mathbf{T}_a - \mathbf{S}(\mathbf{K}^{-1}\mathbf{R}) \quad (22)$$

from which the incremental dislocation density amplitudes can be obtained. This method can be used iteratively to determine the tractions along the crack face, and finally to calculate the stress intensity factors at the crack tips which correspond to the total loads.

Traction Transfer Across Cracks in Concrete

The behavior of concrete changes significantly once cracks form. A wide range of experiments have been performed to study the stresses and relative displacements in the crack and the ultimate strength of the material in the vicinity thereof. The majority of these experimental results were aimed at shear transfer in cracks in both reinforced and plain concrete. Comprehensive summaries of these studies are available in the work by Jimenez-Perez, Gergely and White (26) Walraven (37), and ASCE (1). Limited experimental results are available on pure tension in cracks, which can exist immediately after cracking (14,22). After reviewing the basic phenomena of traction transfer in cracks, a few numerical models are referred to, which can be used to represent the constitutive behavior of cracks.

Tractions Due to Aggregate Interlock.—The formation of cracks in concrete has a major influence on the behavior of the material. The conventional approach to accommodate this new stiffness is to reduce the shear and axial stiffness of the material at the points where cracks have formed. A constant reduction factor is typically applied (36) to the uncracked shear stiffness of the material. For cases where the shear resistance is critical, Cedolin and Dei Poli (9) suggested a varying reduction factor as a function of the strain normal to the crack. Other empirical equations for the shear stiffness (which also takes into account the concrete strength) are summarized by Jimenez-Perez, Gergely and White (26). Fenwick (17), Houde (25) and Paulay and Loeber (32) proposed methods of calculating the shear stiffness of concrete as a function of the crack width. Experimental results indicate though that the normal stiffness and shear displacement along the crack plane has an effect on shear transfer in a crack. More recent models by Jimenez-Perez, Gergely and White (26), Fardis and Buyukozturk (15,16), Walraven and Reinhardt, (19) and Bazant and Gambarova (5,18,19) incorporate the additional effects of these models. The latter (5,18,19) provides the most descriptive representation of aggregate interlock and shear transfer in cracked concrete.

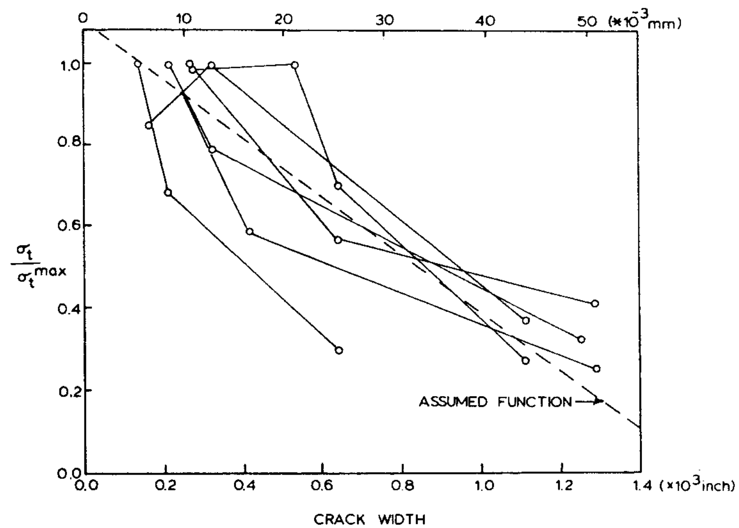

FIG. 4.—Tensile Stresses in Cracks (14)

This formulation can readily be implemented in a nonlinear finite element program. An incremental constitutive relation is assumed for the crack, such that

$$d\sigma_{ni}^{c} = B_{ij} d\delta_j \quad \text{where} \quad i, j = n, t \qquad (23)$$

$d\sigma_{nn}^{c}$ = normal stress in the crack; $d\sigma_{nt}^{c}$ = tangential stress in the crack; $d\delta_n$ = normal relative displacement; $d\delta_t$ = tangential relative displacement; and B_{ij} = empirical stiffness along the crack. This relation should be path-dependent, but due to the lack of sufficient experimental data, it is assumed that

$$\sigma_{nn}^{c} = f_n(\delta_n ; \delta_t) \quad \text{and} \quad \sigma_{nt}^{c} = f_t(\delta_n ; \delta_t) \qquad (24)$$

The constants for the constitutive relation are then

$$B_{nn} = \frac{\partial f_n}{\partial \delta_n}; \quad \text{etc.} \qquad (25)$$

Explicit expressions for the stresses in terms of the relative displacements (Eq. 24) were obtained by Bazant and Gambarova (5,18,19) from the experimental results of Paulay and Loeber (32).

Normal Tractions.—Reported investigations on the tensile cracking and post failure behavior of concrete are limited. Evans and Marathe (14) constructed a very stiff testing frame and was able to control the test specimens after cracks formed under tensile loading. The uniaxial stress-strain relations were recorded with strain gages and the width of the cracks were measured with optical microscopes. The stresses as measured at different crack widths are presented in Fig. 4. Specific details regarding the depth of the cracks, their distribution, the presence of other microcracks and the aggregates used are not available. It is also not clear whether the reduction in stress can solely be ascribed to the increase in crack width, or whether the crack growth (through the specimen thickness) could be the reason for this softening.

Heilmann, Hilsdorf and Finsterwalter (22) subjected long prisms to both concentric and eccentric tensile loads. By attaching several strain gages to each face of a specimen, it was possible to measure the strain at several points along its length, and also around its circumference. In most cases a crack formed within a region covered by a strain gage, and it was possible to record the strain over the crack. The measured stress-strain relations for two of the tests are given in Fig. 5 (the numbers in parentheses in the stress-strain relation refer to the strain gages on the specimen). Notice for example that the slope of the unloading branch for gages 4, 7 and 10 are approximately the same as the loading branch (the specific stress levels, and the implied residual strains for these positions can possibly be ascribed to the dynamic behavior of the specimen during the abrupt failure and unloading). It can then be assumed that the material remained essentially linear in those areas where a crack did not form. From the available information it seems as though only one single crack formed. No mention is made of any microcracks or residual secondary cracks. However, Mindess and Diamond (29) found that, should a region of microcracks form prior to crack propagation, some of these cracks coalesce to form the main crack, while others close again. If that was the case for this crack, the material adjacent to the crack can also

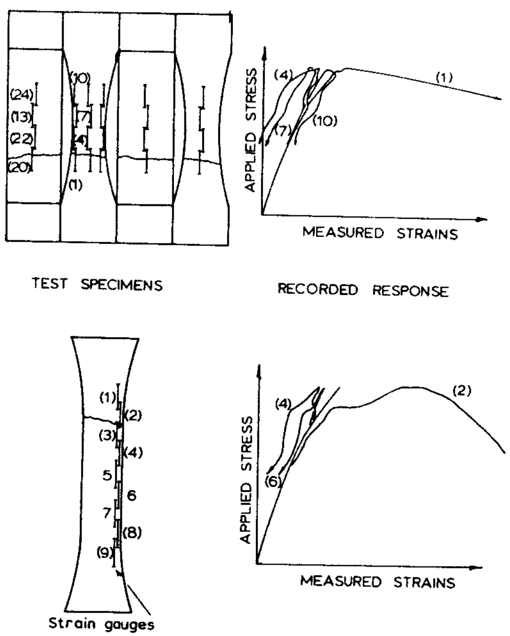

FIG. 5.—Experimental Results of Tractions in Cracks under Tensile (22)

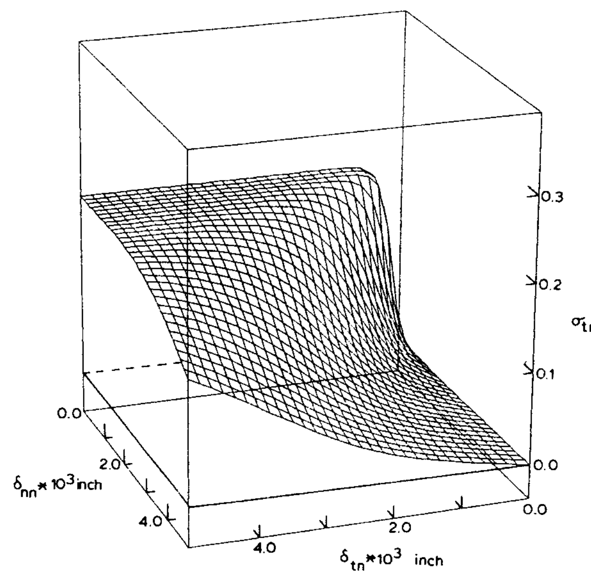

FIG. 6.—Shear Stresses in Crack

be regarded as linearly elastic (or nearly so), and would have unloaded similarly. In that case, the large increase in strain across the crack was caused by the increase in crack width, as measured by the strain gage. After the necessary adjustments have been made for the elastic material adjacent to the crack, these stress-strain relations can be used to find the relation between stress and crack opening. The resulting "crack strain" should then be multiplied by the strain gage length to obtain the crack opening. By studying the results of these experiments, it also becomes clear that, even under pure tensile loads, the material does not debond instantaneously through the full thickness of the specimen, but propagates through the thickness. Certain ligaments tend to remain unbroken (29) and aggregates span the crack (8), which ensure that the stress does not instantaneously drop to zero. These aspects seem to support the experimental results previously reviewed. Due to the lack of reliable data, it will be assumed that a linear law will be sufficient to represent the basic properties. It can be assumed that the average aggregate size in the concrete will influence this softening law, but no experimental data is available to verify this. The proposed relation between stress and crack width is given by the straight line in Fig. 4.

Constitutive Relations Along Crack.—The expressions proposed by Bazant and Gambarova (5,18,19) are based on tests performed on precracked concrete specimens (32). No attempt has been made to represent the transition from the originally uncracked material to the cracked condition. No test data is available from which any numerical model can be derived. The two aforementioned models have been combined in one general constitutive law which describes the basic characteristics of a crack under pure mode I (opening) or mixed mode crack displacements. The basic concepts are briefly reviewed later.

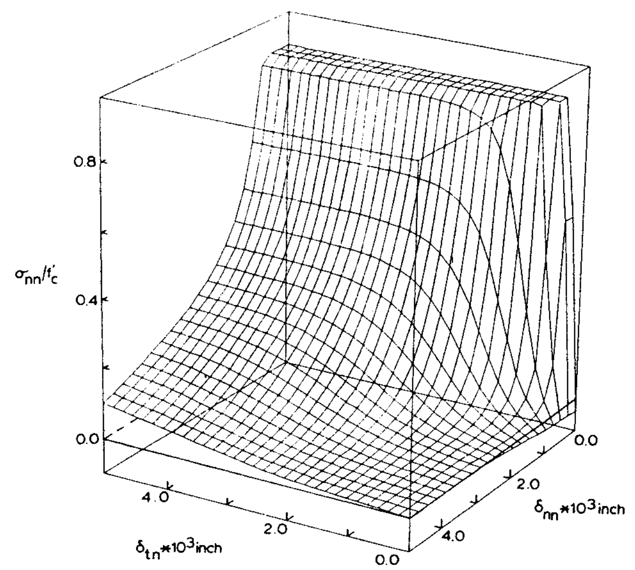

FIG. 7.—Normal Stress In Crack

The concrete in the cracked condition can be represented by the Bazant-Gambarova model. Specific attention has to be given to the initial condition when the crack starts to open. Aggregate interlock prevents any shear displacement in a crack of zero width, so that only opening displacements can occur initially. The Bazant-Gambarova model exhibits this trend, but becomes singular at zero normal displacements. For that reason it is assumed that, for all displacements less than a certain opening, the shear stiffness will be constant, and the normal stiffness will have two constant components from the shear transfer model and the normal traction model. Beyond this minimum opening the two models are superimposed. Graphical representations of the material model are given in Figs. 6 and 7, in which the shear stresses and normal stresses are plotted against the relative shear and normal crack displacements.

Simulation of Experimental Results

The hybrid method described before was incorporated in a finite element program which has 8 node isoparametric elements for plane stress and plane strain analyses. This program was used to analyze a notched beam specimen tested at Cornell University (3) (refer to Fig. 8). Two sets of analyses were performed for the same plain concrete beam (beam type C in the tests). The first series of results were obtained from a linear elastic analysis in which it was assumed that no shear transfer occurred across the crack. In the second series the nonlinear shear transfer model was used to obtain a few data points.

The crack path was determined by initially specifying the saw cut notch as part of the crack. A short additional crack length (probe) was added to the notch, and its direction with respect to the notch varied so that the value of K_{II} was zero at the crack tip. From that point on, the program was allowed to calculate the direction of any crack extension from the values of K_I and K_{II} at the crack tip. The path obtained from this procedure is given in Fig. 9, as well as the limits within which the experimental results lay. It can be expected that any further extensions will also fall within the range of the tests, since the shear stresses have (in the vicinity of the current tip) been reduced substantially, and K_{II} can be expected to remain small along the path.

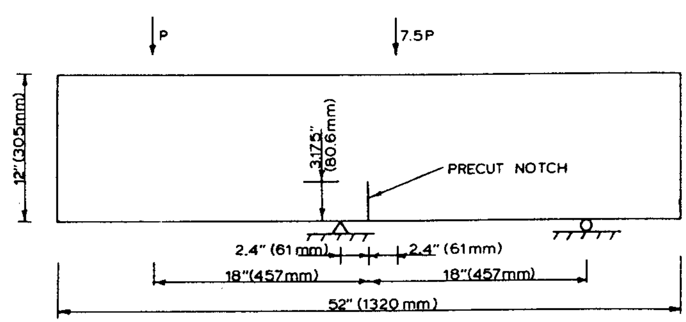

FIG. 8.—Layout of Test Beam

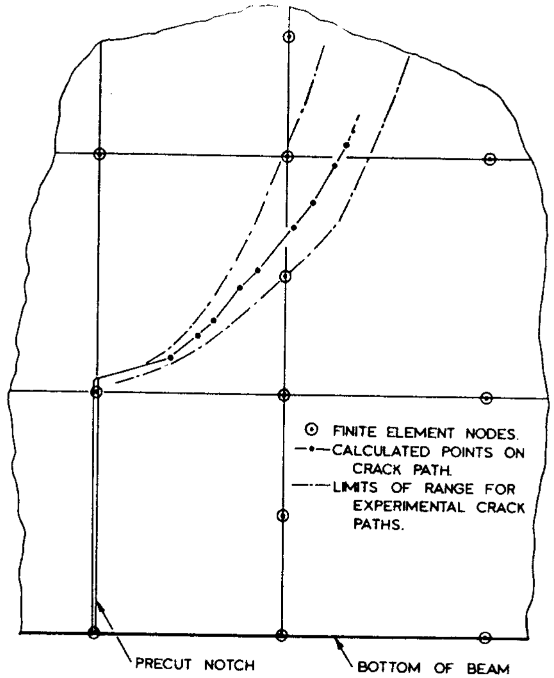

FIG. 9.—Calculated Crack Path

The loads corresponding to each crack length were obtained by calculating the magnitude of the load which would make K_I equal to K_{IC}. Experimentally obtained values for K_{IC} of 726 psi $\sqrt{\text{inch}}$ (25.2 MPa $\sqrt{\text{mm}}$) and the initial modulus of elasticity of 3,600 ksi (24.8 GPa) were used in the numerical calculations. Note that the loads are considerably below the experimentally obtained loads. This can largely be attributed to the lack of any traction transfer model for the crack. Shear transfer would tend to resist the sliding of the two crack faces over each other, while any residual tensile strength would tend to prevent it from opening. This will have the effect of reducing the value of K_I, so that the load that the specimen can carry with any particular crack length would increase. A few points were calculated with the traction transfer model, and the results are given in Fig. 10. The critical stress intensity factor method was also used for these analyses. It was found that the area in which the asymptotic stresses exceeded the tensile strength of the material was small, so that the assumed linear elastic crack tip field did not significantly effect the fracture analysis. An alternative method would be to enforce a zero stress intensity factor (K_I) at the tip, and to use energy considerations (e.g. J-integral) as a propagation criteria. It is anticipated that the traction transfer model will not change the crack path significantly.

In the linear elastic analyses (without any crack tractions), the system of equations (Eq. 9*a*) was solved directly without taking advantage of

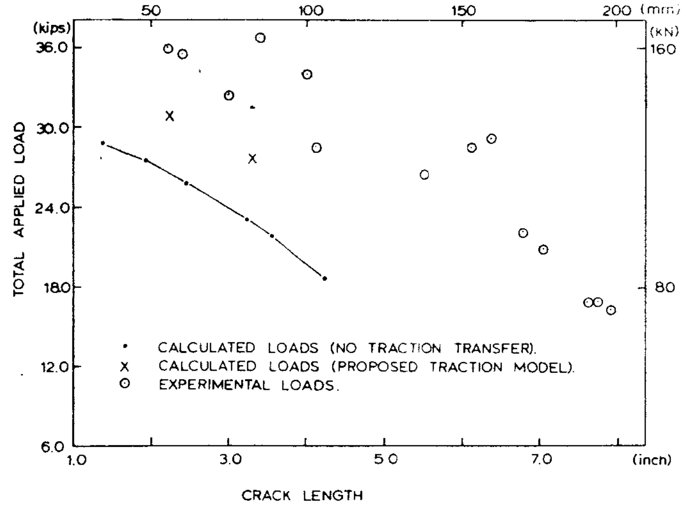

FIG. 10.—Calculated Applied Loads

any bandedness or symmetry of the finite element stiffness matrix (**K**). For the model with 85 finite element nodes and 19 integration points along the crack, the total CPU processing time on a VAX 11-782 computer was approximately 55 sec. With the decoupled method, the initial **K** matrix decomposition and backsubstitution ($\mathbf{K}^{-1}\mathbf{R}$) need not be done for subsequent steps, so that the time per step can be reduced by approximately 25% per load step (it was found that the VAX 11-782 computer is approximately 2–3 times slower than an IBM 370-158).

Conclusion

A method is proposed for the analysis of discrete cracks in concrete which accounts for aggregate interlock in the crack. The body around the crack is treated as a linearly elastic, isotropic material, and represented by finite elements. The crack is modeled by dislocations distributed along the length of the crack. A numerical model, which was derived from experimental data, represents the properties of the material along the crack. This method was used to analyze a beam subjected to mixed mode fracture. The calculated crack path was within the experimentally obtained range. Although the load history was slightly below the experimental values, the general trend was satisfactory and matched the reduction in load with increasing crack length. The difference in load is attributed to the approximations inherent in the adopted aggregate interlock behavior.

Nonlinear response of concrete structures can be ascribed to the nonlinear stress-strain behavior of the material, effects of crack formation and propagation on the overall response, and the nonlinearities involved in traction transfer across the cracks. The proposed method can accommodate the latter two sources of nonlinearities associated with cracks. Under tensile stresses concrete behaves in a brittle manner and fails before any significant plastic yielding takes place. When cracks form, the gradual softening of the material introduces additional nonlinear behavior, which can satisfactorily be modeled by the constitutive relations of the material in the cracks.

The current method is only valid for specimens in which the material (other than that in the crack region) remains linearly elastic. This approximation would be acceptable in many cases when the compressive stress levels remain low. An example is an unreinforced beam in bending (with point or distributed loads) which cracks in a pure mode I manner. In cases where the material does not remain linear, the method, as described here would predict stiff behavioral response. The present model can be modified to accommodate material nonlinearities. For cases where the material immediately adjacent to the crack remains linear, the crack and a certain amount of material around it can be modeled as an elastic substructure of the complete body where only material outside this region has nonlinear properties. Alternatively, all the material can be assigned nonlinear properties, in which case the presently adopted stress and displacement influence functions will introduce inaccuracies. Nevertheless, preliminary investigations have shown that the latter generalization provides satisfactory results for practical purposes.

A major advantage of the hybrid method is that no remeshing of the finite elements is required upon crack propagation, since the finite elements represent the intact body, while the distribution of dislocations represent the crack. Apart from removing the necessity of any user intervention during an analysis, the nonlinear stress histories at finite element integration points can be used directly, and no interpolation schemes would have to be devised to transfer these histories from one finite element configuration to the next (3,8) when nonlinear material properties are used.

It is envisaged that the present method can be used in the analysis of local details of large structures to investigate the stability and resistance against failure. Specific examples are the tensile failure of concrete at embedded brackets and bolts, and the crack propagation at local stress concentrations in prestressed members.

Further extensions to the current model would be to include the dowel effects of reinforcing bars in the constitutive model for the crack, and also to incorporate the cyclic behavior of the shear transfer model in a crack. The reinforcement can be represented by single bar elements, while the crack interface properties have to be modified at the bar to represent any dowel and tension stiffening effects.

Acknowledgments

The assistance and advice of Michael Cleary and Bal Annigeri are greatly appreciated.

Appendix I.—References

1. "Finite Element Analysis of Reinforced Concrete," American Society of Civil Engineers, New York, N.Y., 1982.
2. Annigeri, B. S., and Cleary, M. P., "Surface Integral Finite Element Hybrid (SIFEH) Method for Fracture Mechanics," *Report No. REL-82-21*, Department of Mechanical Engineering, Massachusetts Institute of Technology, Cambridge, Mass., 1982.
3. Arrea, M., and Ingraffea, A. R., "Mixed-Mode Crack Propagation in Mortar and Concrete," *Report No. 81-13*, Department of Structural Engineering, Cornell University, Ithaca, N.Y., Feb., 1982.
4. Bazant, Z. P., and Cedolin, C., "Blunt Crack Band Propagation in Finite Element Analysis," *Journal of the Engineering Mechanics Division*, ASCE, Vol. 105, No. EM2, 1979, pp. 297–315.
5. Bazant, Z. P., and Gambarova, P., "Rough Cracks in Reinforced Concrete," *Journal of the Structural Division*, ASCE, Vol. 106, No. ST4, 1980, pp. 819–842.
6. Bazant, Z. P., and Oh, B. H., "Concrete Fracture via Stress-Strain Relations," *Report No. 81-10/665c*, Center for Concrete and Geomaterials, Northwestern University, Evanston, Ill., 1981.
7. Carpenteri, A., "Application of Fracture Mechanics to Concrete Structures," *Journal of the Structural Division*, ASCE, Vol. 108, No. ST4, 1982, pp. 833–848.
8. Catalano, D. M., and Ingraffea, A. R., "Concrete Fracture: A Linear Elastic Fracture Mechanics Approach," *Report No. 82-1*, Department of Structural Engineering, Cornell University, Ithaca, N.Y., 1982.
9. Cedolin, L., and Dei Poli, S., "Finite Element Studies of Shear Critical R/C Beams," *Journal of the Engineering Mechanics Division*, ASCE, Vol. 103, No. EM3, 1977, pp. 3935–410.
10. Cleary, M. P., "Continuously Distributed Dislocation Model for Shear-Bands in Softening Materials," *International Journal of Numerical Methods in Engineering*, Vol. 10, No. 3, 1976, pp. 679–702.
11. Cleary, M. P., "Moving Singularities in Elasto-Diffusive Solids with Applications to Fracture Propagation," *International Journal of Solids and Structures*, Vol. 14, No. 2, 1978, pp. 81–97.
12. Dugdale, D. S., "Yielding of Steel Plates Containing Slits," *Journal of the Mechanics and Physics. Solids*, Vol. 8, 1960, pp. 100–108.
13. Erdogan, F., and Sih, G. C., "On the Crack Extension in Plates under Plane Loading and Transverse Shear," *Journal of Basic Engineering*, Vol. 85, No. 12, 1963, pp. 819–527.
14. Evans, R. H., and Marathe, M. S., "Microcracking and Stress Strain Curves for Concrete in Tension," *Materials and Construction*, Vol. 1, No. 1, 1968, pp. 61–64.
15. Fardis, M. N., and Buyukozturk, O., "A Shear Transfer Model for Reinforced Concrete," *Journal of the Engineering Mechanics Division*, ASCE, Vol. 105, No. EM2, 1979, pp. 155–275.
16. Fardis, M. N., and Buyukozturk, O., "Shear Transfer of Concrete by Finite Element," *Journal of the Structural Division*, ASCE, Vol. 106, No. ST6, 1980, pp. 1311–1327.
17. Fenwick, R. C., "The Shear Strength of Reinforced Concrete Beams," thesis presented to the University of Canterbury, Christchurch, New Zealand, in 1966, in partial fulfillment of the requirements for the degree of Doctor of Philosophy.
18. Gambarova, P., "In Aggregate Interlock Mechanism in Reinforced Concrete Plates with Extensive Cracking," presented at the IABSE Colloquium Delft, The Netherlands, 1981, pp. 105–133.
19. Gambarova, P., "A Tentative Formulation of the Stress-Displacement Relations for Aggregate Interlock in the Case of Repeated Loads," presented at the ASCE Spring Convention, April 16–30, 1981, Las Vegas, Nev., 1982.
20. Gylltoft, K., "Fracture Mechanics Models for Fatigue in Concrete Structures," thesis presented to Lulea University of Technology, at Lulea, Sweden in 1983, in partial fulfillment of the requirements for the degree of Doctor of Philosophy.
21. Griffith, A. A., "The Phenomena of Rupture and Flow in Solids," *Philosophical Transaction of the Royal Society of London*, Series A, No. 221, 1920, pp. 163–198.

22. Heilmann, H. G., Hilsdorf, H., and Finsterwalder, K., "Festikeit und Verformung von Beton unter Zugspannungen," *Deutches Ausshus fur Stahlbeton*, Part 203, Von Wilhelm Ernst and Son, Berlin, Germany, 1969.
23. Hirth, J. P., and Lothe, J., *Theory of Dislocations*, McGraw-Hill, New York, N.Y., 1968.
24. Hillerborg, A., Modeer, M., and Petersson, P. E., "Analysis of Crack Formation and Crack Growth in Concrete by Means of Fracture Mechanics and Finite Elements," *Cement and Concrete Research*, Vol. 6, No. 6, 1976, pp. 773–781..
25. Houde, J., "Study of Force-Displacement Relationship for the Finite Element Analysis of Reinforced Concrete," *Structural Concrete Series*, No. 73-2, McGill University, Montreal, Canada, 1973.
26. Jimenez-Perez, R., Gergely, P., and White, R. N., "Shear Transfer Across Cracks in Reinforced Concrete," *Report 78-4*, Department of Structural Engineering, Cornell University, Ithaca, N.Y., 1978.
27. Kaplan, M. F., "Crack Propagation and the Fracture of Concrete," *Journal of the American Concrete Institute*, Vol. 58, No. 5, 1961, pp. 591–609.
28. Kesler, C. E., Naus, D. J., and Lott, J. L., "Fracture Merchanics—Its Applicability to Concrete," presented at the August 15–20, 1971, International Conference on Mechanical Behavior of Materials, in Kyoto, The Society of Materials Science, Japan, Vol. IV, 1972, pp. 113–124.
29. Mindess, S., and Diamond, S., "A Preliminary SEM Study of Crack Propagation in Mortar," *Cement and Concrete Research*, Vol. 10, No. 5, 1980, pp. 509–510.
30. Mindess, S., "Fracture Toughness Testing of Cement and Concrete," Fracture Mechanics of Concrete, edited by F. H. Wittmann, Elsevier Scientific Publishing Co., 1983.
31. Nabarro, F. R. N., "The Mathematical Theory of Stationary Dislocations," *Advances in Physics*, Vol. 1, No. 3, 1952, pp. 269–279.
32. Paulay, T., and Loeber, P. S., "Shear Transfer by Aggregate Interlock," Shear in Reinforced Concrete, Vol. 1, *Special Publication SP-42*, American Concrete Institute, Detroit, Mich., 1973.
33. Petersson, P. E., "Fracture Energy of Concrete: Practical Performance and Experimental Results," *Cement and Concrete Research*, Vol. 10, No. 1, 1980, pp. 91–101.
34. Petersson, P. E., and Gustavson, P. J., "A Model for Calculation of Crack Growth in Concrete-Like Materials," presented at the July 1980, International Conference on Numerical Methods in Fracture Mechancis, held at Swansea, Wales.
35. Saouma, V. E., Ingraffea, A. R., and Catalano, D. M., "Fracture Toughness of Concrete: K_{IC} Revisited," *Journal of the Engineering Mechanics Division*, ASCE, Vol. 68, No. EM6, 1982, pp. 1152–1166.
36. Suidan, M., and Schnobrich, N. C., "Finite Element Analysis of Reinforced Concrete," *Journal of the Structural Division*, ASCE, Vol. 99, No. ST10, 1973, pp. 2109–2122.
37. Walraven, J. C., "Mechanism of Shear Transfer in Cracks in Concrete—A Survey of Literature," *Stevin Report 5-78-12*, University of Technology, Delft, The Netherlands, 1978.
38. Walraven, J. C., and Reinhardt, H. W., "Theory and Experiments on the Mechanical Behavior of Cracks in Plain and Reinforced Concrete Subjected to Shear Loading," *Heron*, Vol. 27, No. 1A, 1981.

Appendix II.—Notation

The following symbols are used in this paper:

B_{ij} = stiffness of material in the crack;
$\mathbf{C}$ = crack traction influence functions due to unit dislocation density amplitudes;

$\mathbf{D}$ = relative crack displacement influence functions due to unit dislocation density amplitudes;
$\mathbf{E}$ = constitutive tangent matrix at integration points along crack;
f = tractions along the crack;
$\mathbf{F}$ = dislocation density amplitudes;
$\mathbf{G}$ = traction influence functions at finite element nodes due to unit dislocation density amplitudes;
$\mathbf{K}$ = stiffness matrix of uncracked specimen;
K_I = Mode I stress-intensity factor;
K_{IC} = critical mode I stress-intensity factor;
K_{II} = Mode II stress-intensity factor;
$\mathbf{L}$ = displacement influence functions due to unit dislocation density a amplitudes;
$\mathbf{R}$ = applied load vector;
$\mathbf{S}$ = crack traction influence function due to unit displacement at finite elements nodes;
$\mathbf{T}$ = tractions along the crack;
$\mathbf{T}_a$ = applied tractions along the crack;
$\mathbf{T}_{cr}$ = tractions along crack due to aggregate interlock and imperfect debonding;
$\mathbf{U}$ = finite element nodes displacements;
$\mathbf{U}_{cr}$ = relative displacements between crack faces;
δ = relative displacements between crack faces;
θ = angle at which the crack propagates;
ϕ = function; and
σ^c = tractions along crack due to aggregate interlock and imperfect debonding.

Subscripts

e = effective;
n = normal; and
t = tangential.

Superscripts

fe = finite element; and
si = surface integral.